Environmental Engineering and Management Journal March 2021, Vol. 20, No. 3, 397-404
http://www.eemj.icpm.tuiasi.ro/; http://www.eemj.eu

"Gheorghe Asachi" Technical University of Iasi, Romania

NON-THERMAL PLASMA T-SHAPED REACTOR FOR ACTIVATED WATER PRODUCTION

Radu Burlică[1], Dragoș Astanei[1]*, Daniel-Eusebiu Crețu[1], Iuliana-Delicia Dîrlău[1], Oana Beniugă[1], Silvica Pădureanu[2], Vasile Stoleru[2], Antoanela Patraş[2]

[1] *"Gheorghe Asachi" Technical University of Iasi, 700050, Iasi, Romania*
[2] *"Ion Ionescu de la Brad" University of Agricultural Sciences and Veterinary Medicine, Iasi, Romania*

Abstract

Non-thermal plasma is an innovative, eco-friendly technology, being considered as an emerging technology in many research fields. This work presents an analysis of the influence of different parameters on the energy efficiency of a T–shaped non-thermal plasma reactor for plasma activated water generation. The tests were performed on four distinct designs (T1, T2, T3, T4) of this type of reactor for which the following input parameters were varied: frequency (60, 150 and 250 Hz), water flows (5, 10, 15 and 20 mL/min) and gas flows (1 and 2 L/min Ar). It has been shown that the configurations T3 and T4, whose discharge is generated between the gas inlet and outlet electrode, are less efficient compared to designs T1 and T2, where the discharge is generated between the water inlet electrode and the outlet electrode. It was also considered the influence of the polarity of the pulse power supply where the reverse polarity (T2 design) records significant values at the gas flow of 1 L/min. The carrier gas was argon, which has been chosen in order to avoid radical quenching reactions by other molecular species, such as nitrates and nitrites, generated in the atmospheric air plasma.

Key words: energy efficiency, hydrogen peroxide, non-thermal plasma, plasma-activated water

Received: June, 2020; Revised final: August, 2020; Accepted: January, 2021; Published in final edited form: March, 2021

1. Introduction

Non-thermal plasma (NTP) represents a new technology used, in present, for a wide range of applications. It has already been demonstrated to be effective in applications such as surface treatment (Astanei et al., 2016), degradation or conversion of organic pollutants from aqueous solutions (Brisset et al., 2016; Moussa and Brisset, 2003; Moussa et al., 2007) or the treatment of air and polluted water (Burlica et al., 2019; Ursache et al., 2015; Zadi et al., 2018;). There are also applications of NTP in medicine (e.g. wound treatment) (Kramer et al., 2017), hydrogen generation (Burlica et al., 2011), surface sterilization or in agriculture (Stoleru et al., 2018).

Advantages of the technology have been proved to be effective in the field of plants growth in agriculture, enhancing the bio-mass production rate. It also reduces the time window of the plant growth until maturity and provides organic fertilizer for plants, and in the same time it assures bacterial/fungicide protection (Burlica et al., 2010; Gomiero et. al., 2008; Vitousek et al., 1997). The innovative technologies that uses NTP represent an ecological and non-stressful plants treatment method ant it can be used in two different directions:

- the first one, refers to the direct treatment of the seeds, in order to enhance their germination rate and to protect them against pathogens (e.g. fungi) (Kriz et al., 2016; Sera et al., 2013).
- the second direction, is represented by the indirect treatment throughout the means of plasma activated water (PAW), which acts as disinfection agent, due to the presence of hydrogen peroxide

* Author to whom all correspondence should be addressed: e-mail: dragos.astanei@tuiasi.ro; Phone: +40767452144

(H_2O_2). In the same time it stands as bio-fertilizer, due to the nitrogen species induced by plasma treatment in water (Bafoil et al., 2018; Padureanu et al., 2018; Sivachandiran and Khacef, 2017).

The interaction of plasma with water droplets leads to the formation of hydrogen peroxide and hydroxyl radicals, due to the electron's "bombardment" of water molecules. The H_2O_2 formed in water acts as a disinfection agent on the plants leaves (inactivates the pathogen microorganisms). In order to characterize the reactors capabilities to produce PAW the argon have been used as a carrier gas, in order to form a homogeneous discharge due to the fact that argon is an easy ionised gas (the ionisation energy is low – starting from1520.57 kJ mol^{-1}).

The water treatment with plasma in Ar as the carrier gas, along of hydroxyl radical (•OH), active argon ions and free electrons are generally the main reactive species responsible for the reactive species produced in PAW (Bian et al., 2007; Clyne et al., 1969; Siddique et al., 2011), Eq. (1-4).

$$e^- + \bullet Ar \rightarrow Ar^* + e \quad (1)$$

$$e^- + Ar \rightarrow Ar^+ + e^- + e \quad (2)$$

$$Ar^+ + H_2O \rightarrow Ar^+(H_2O) \quad (3)$$

$$Ar^+(H_2O) + H_2O \rightarrow H_3O^+ + \bullet OH + Ar \quad (4)$$

The interaction between water and plasma leads to the direct formation of the •OH radicals mostly due to the free electrons and Ar ions interaction with water molecules. The formation of the •OH radicals leads to the generation of the hydrogen peroxide, as shown in (Eq. 5-7) (Brisset et al, 2008; Hnatiuc et al., 2012; Locke and Shih, 2011):

$$H_2O \rightarrow H + OH \quad (5)$$

$$H + H \rightarrow H_2 \quad (6)$$

$$OH + OH \rightarrow H_2O_2 \quad (7)$$

This work is focused on the study of T-shaped NTP reactor for PAW production, which further is used on plants irrigation, in germination and growing process.

The aim of this study is analysing the influence of different parameters (frequency, gas and water flow rate) on the hydrogen peroxide formation and energy efficiency of a T–shaped NTP reactor for PAW generation. Moreover, the study follows the influence of the polarity of the pulse power supply for different values of pulse frequencies, gas and water flow rates.

2. Experimental

The proposed technical solution to produce PAW is a T-shaped reactor (T-NTP), consisting of three ports (Fig. 1), two inlets, one for water and the other for gas, and an outlet for PAW, which comes out as a spray. This new solution assimilates the technique of spraying water throughout a two-port nozzle into a simple, robust system, where the mixture of water and gas is made directly into the plasma area Fig.1(a). In this case, the electric discharge produced in the reactor chamber by high voltage pulses is generated between two of the electrodes. The reactor body dimensions are 25 mm x 20 mm. The electrodes have a length of 40 mm and the inner diameter was 0.2 mm. The novelty of the proposed solution is that the mixture between water and gas is made directly into the narrow chamber of the reactor where the plasma is also generated.

The T-NTP reactor is supplied by a high voltage pulsed power supply (HVPS) that generates a low power electrical discharge, between two of the reactor's electrodes Fig. 1(b). A pump injects the water perpendicularly on the gas flow direction. This assures a higher interaction between the plasma and the water. The low power of the plasma does not increase significantly the temperature of the water droplets in the reactor, and therefore, enhances the energy yields for H_2O_2 production due to suppression of quenching reactions of radicals with other molecular species.

Initially, pure water has been sprayed into the reactor, and H_2O_2 (when Ar is used as carrier gas) has been measured using colorimetric methods based on titanyl sulphate ($TiOSO_4$) which acts as a reagent. The colour of the testing solution turns to yellow in the presence of the H_2O_2.

The experiments have been performed on four distinct configurations of the T-NTP reactor (Fig. 2), as presented below:

- T1 direct polarity configuration (design), where the high voltage (HV) is connected to the water inlet electrode, while the PAW output electrode is grounded;
- T2 configuration with reverse polarity, where the HV is connected to the PAW output electrode, while the water input electrode is grounded;
- T3 direct polarity configuration, where the HV is connected to the gas inlet electrode (Ar) positioned on the side of the reactor, while the outlet electrode is grounded;
- T4 configuration with direct polarity, where the HV is connected to the gas input electrode (Ar), while the output electrode is connected to the ground.

The distance between the electrodes was set to 3 mm. For this experiment, three frequency values of 60, 150 and 250 Hz have been considered for a constant pulse width of 2 ms.

The distilled water is injected directly in the plasma region by a pump into the gas flow. This ensures a greater interaction between plasma and water droplets. The gas and water were mixed into the reactor, throughout two-inlet nozzle directly into the plasma area. Argon was chosen as a carrier gas to avoid generation of other molecular species than H_2O_2, molecular species that could interact with the hydrogen peroxide and decrease its concentration. For the tests, four values of the flow rates of demineralized water of 5, 10, 15 and 20 mL/ min and two gas flows of 1 and 2 L/min were considered. The electric discharge parameters were recorded using a high-resolution Lecroy 454 digital oscilloscope (OSC). The voltage was measured using a high voltage probe - HVP with a ratio of 1:1000 (Fig. 2) while the current was assessed using a shunt of 100 Ω (SH). Typical waveforms of current, voltage and control recorded are illustrated in Fig. 3.

The waveforms correspond to the following experimental conditions: frequency 150 Hz, direct polarity (DP), gas flow 1 L/min, water flow 20 mL/min. Based on the acquired waveforms for voltage and current, the average power and energy per discharge were calculated. The measurement made based on the current and voltage waveforms have an approximate error of ±5%. The H_2O_2 concentration was determined using a colorimetric method based on titanium sulphate as reagent. The absorption spectra of the solution, recorded by a Shimadzu UV-VIS Mini 1240 spectrophotometer, provide peaks proportional to the H_2O_2 concentration for the wavelength λ_{H2O2} = 410 nm.

In order to verify the experiments repeatability and to ensure significant results, 5 to 15 sets of tests have been performed for each experimental conditions considered. The standard average deviation of the obtained results determined for 15 sets of tests performed for the same experimental conditions is lower than 5%. For each determination of H_2O_2 concentration (2 mL PAW and 1 mL $TiOSO_4$ mixed into a standard quartz cell), at least 3 repetitions have been performed for each test.

For a complete assessment of the influence of polarity on the parameters of PAW, the energy efficiency *EEf* [g/kWh] has been considered. *EEf* was calculated using (Eq. 8):

$$EEf = \frac{[H_2O_2] \cdot v_0}{1000 P_{med} \cdot t} \qquad (8)$$

where: *EEf* is energy efficiency [g/kWh], $[H_2O_2]$ is the concentration of hydrogen peroxide [mg/L], v_o represents the volume of the solution generated [L], P_{med} represents the average discharge power [kW], and *t* is the time required to produce 20 ml of PAW.

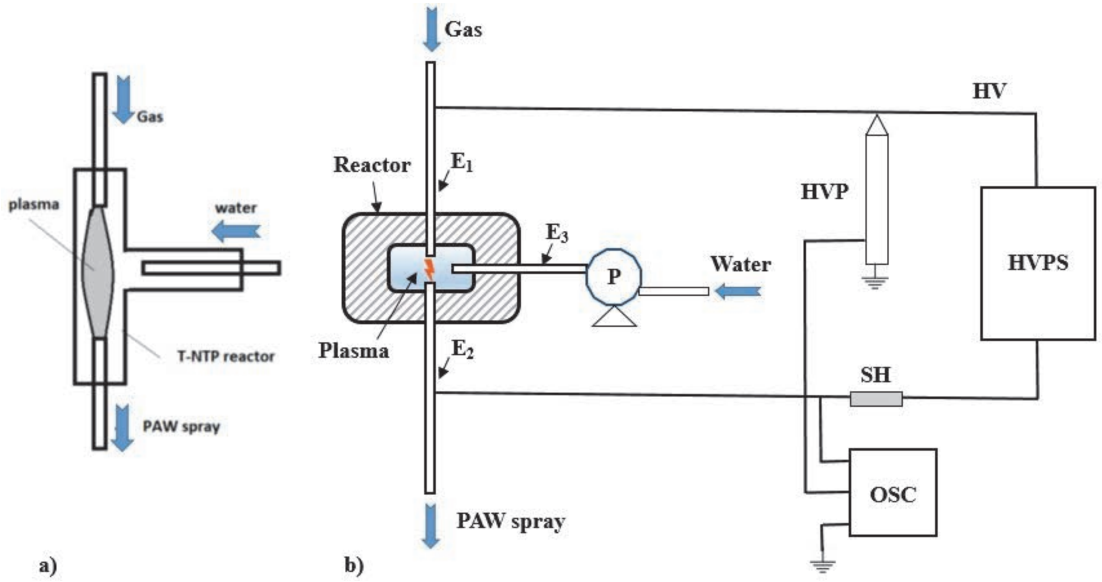

Fig. 1. a) The T-NTP reactor geometry; b) – the electrical schematic

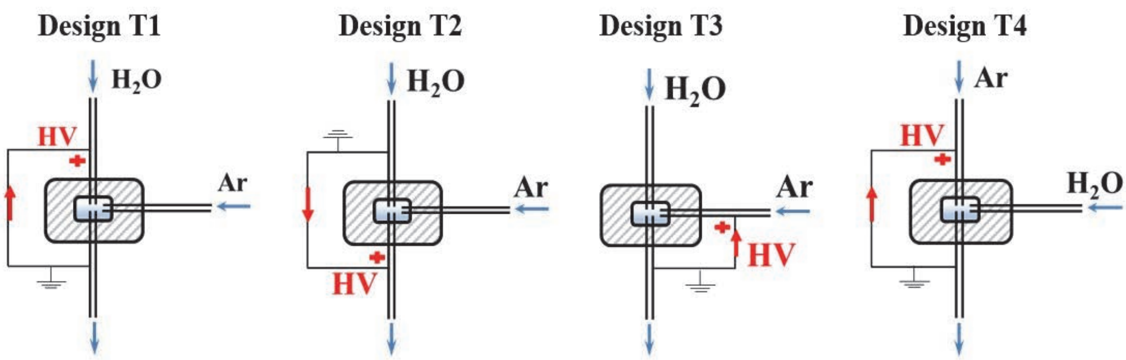

Fig. 2. Experimental set-up configurations of T-NTP reactor

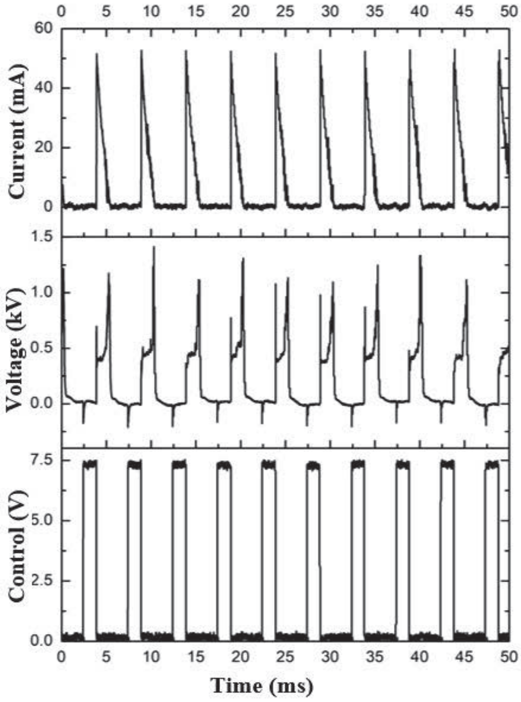

Fig. 3. Current and voltage waveforms

3. Results and discussion

In order to determine the optimum configuration of the T-NTP reactor for PAW production, it was assessed the H_2O_2 concentration and energy efficiency, while the Ar was used as working gas. The average power values are presented in Table 1 for the considered frequencies and gas flow rates. The discharge power is increasing with the frequency due to a higher duty cycle – the control pulse width was kept constant at 2 ms, the most notable values being achieved at 250 Hz.

In T1 design, the water flow is injected through the HV electrode (+), so that the electrons emitted by the outlet electrode (-) result in a mixture of gas-liquid, where Ar is prevalent. In T2 design the water flow is injected through the (-) electrode resulting in a low electrons emission because the water is prevalent in the reactor chamber.

The differences between T1 and T2 are because the initiation of the discharge takes place in different electrical conditions, as a result of different gas-liquid mixture physical parameters (injection ports and direction, gas velocity).

In T3 configuration, the Ar gas flow is injected perpendicularly on the discharge, favouring the discharge shut down due to the cooling effect (deionization of excited particles) of the plasma channel.

In T4 design the water injected in the gas stream flooded the (-) electrode therefore electrons emission from the (–) electrode is diminished. In this case only a part of the amount of energy provided by the power supply is transferred to the plasma. Differences in the order of (W) units between configurations are important.

The highest average power within the 4 configurations has been measured for T1, where the discharge is generated between the water inlet and outlet electrodes, the polarity being considered direct.

Table 1. The average power of the T-NTP reactor discharge vs. frequency

Reactor design	*Average Power [W] (average for the all 4 values of water flow rates)*					
	1 [L/min] Ar			*2 [L/min] Ar*		
	60 Hz	*150 Hz*	*250 Hz*	*60 Hz*	*150 Hz*	*250 Hz*
T1 design	1.08	3.85	5.28	1.36	3.13	4.46
T2 design	0.90	2.74	4.20	1.13	2.79	3.57
T3 design	1.33	2.87	3.94	1.22	2.65	3.74
T4 design	0.99	2.37	2.97	1.13	2.25	3.24

The concentration of H_2O_2 have been measured for different frequencies, gas and water flow rates. The variation of H_2O_2 concentration in water with the water flow rate, for 250 Hz frequency is presented in Fig. 4. The H_2O_2 concentration decreases with the increase of water flow rate for all configurations considered. This is due to a lower residence time of water droplets in the plasma region, which involves a lower reactive chemical conversion. For the frequency of 250 Hz, at the 1 L/min Ar and the water flow rate 5 mL/min, the concentration of H_2O_2 in the case of T2 design is more than 5 times higher than the values recorded for T4 design, as is illustrated in Fig. 4.

The T3 and T4 reactor configurations leads to lower concentrations of H_2O_2 comparative to the cases where the discharge occurs between the water injection port electrode and the outlet electrode of PAW, either direct polarity (T1) or reverse polarity (T2).

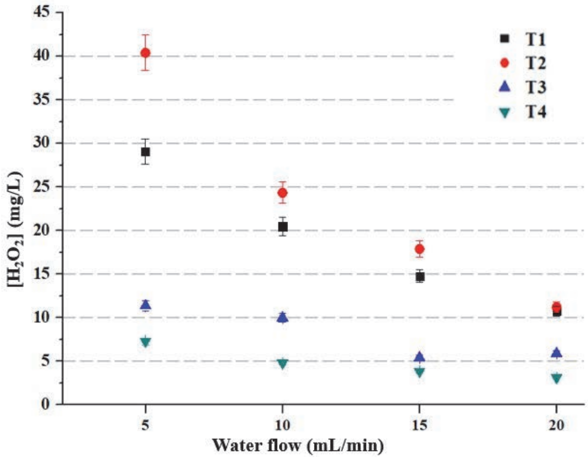

Fig. 4. T-NTP evolution of H_2O_2 concentration at 250 Hz frequency for 1 L/min gas flow rate

At the highest considered frequency, 250 Hz, as well as at 150 Hz, T2 reactor design, records higher values of the concentration relative to the T1 connection, for 1 L/min gas flow. The concentration of H_2O_2 in the case of T1 reactor design increases with the gas flow rate, while for the case of the T2 connection, the H_2O_2 concentration decreases insignificantly (Fig. 5). For the configurations T3 and T4 the H_2O_2 concentration has lower values compared with the previous configurations converging to the same values.

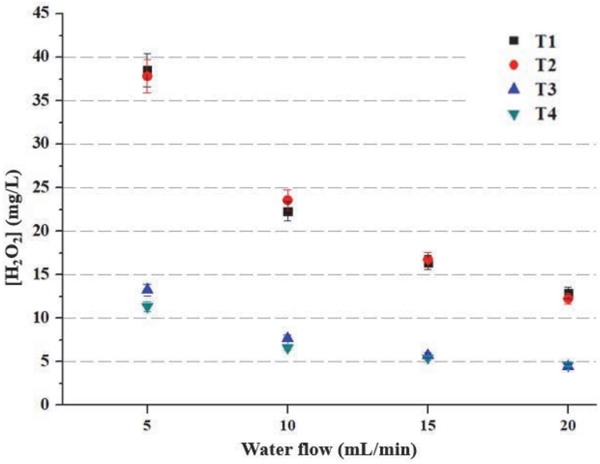

Fig. 5. T-NTP evolution of H_2O_2 concentration at 250 Hz frequency for 2 L/min gas flow rate

In Fig. 6 and Fig.7, the concentration of hydrogen peroxide variation with the frequency, at 5 mL/min water flow rate, are presented.

It has been previously shown that the water flow rate of 5 mL/min has the highest values for H_2O_2 concentration. T2 design shows the most significant concentration, 40 mg/L, at the gas flow rate of 1 L/min, while for T1 design the concentration evolves with the increasing of the working gas flow rate reaching a maximum value of 38 mg/L. The H_2O_2 concentration is increasing with the frequency due to a higher average power, which also means a higher ionization degree of particles in the plasma area.

As previously demonstrated (Locke and Shih, 2011), the energy yield for hydrogen peroxide produced by water–plasma reactions, in different environments, is within 0.5-5 g/kWh, in the case of reactors with fine water droplets sprayed into the low power plasma with argon as carrier gas.

For a complete assessment of the influence of the reactor's configurations on the parameters of PAW, the energy efficiency *EEf* [g/kWh] has been considered. It expresses the amount of H_2O_2 (in grams) induced in the PAW per kWh. Table 2 integrates all the energy efficiency information resulting from the tests performed for reactors in configurations T. The influence of water and gas flow rate, frequency, polarity and different geometries in the modification of *EEf* was also analysed.

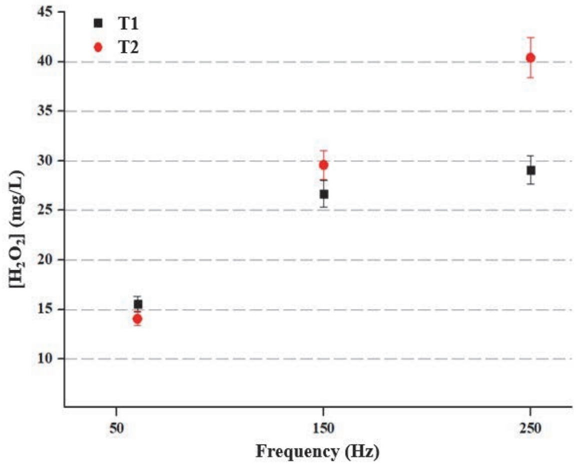

Fig. 6. Evolution of H_2O_2 concentration by frequency for 1 L/min gas flow rate

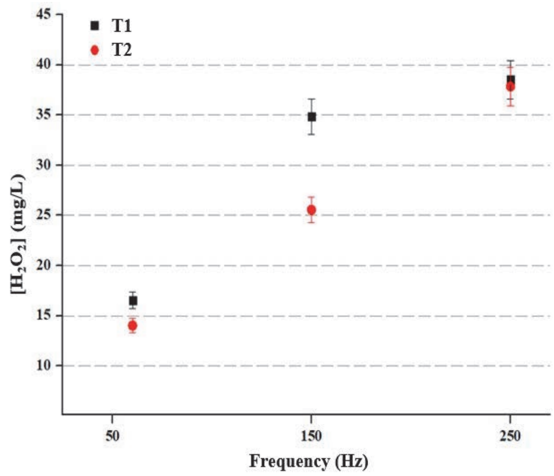

Fig. 7. Evolution of H_2O_2 concentration by frequency for 2 L/min gas flow rate

A comparison between the four configurations of the T-NTP reactor is presented in Fig. 8 with the water flow rate. Similar, as in previous results presented, the configurations T3 and T4 correspond to the lowest values for the energy efficiency, even three times lower than the maximum recorded by the T2 configuration.

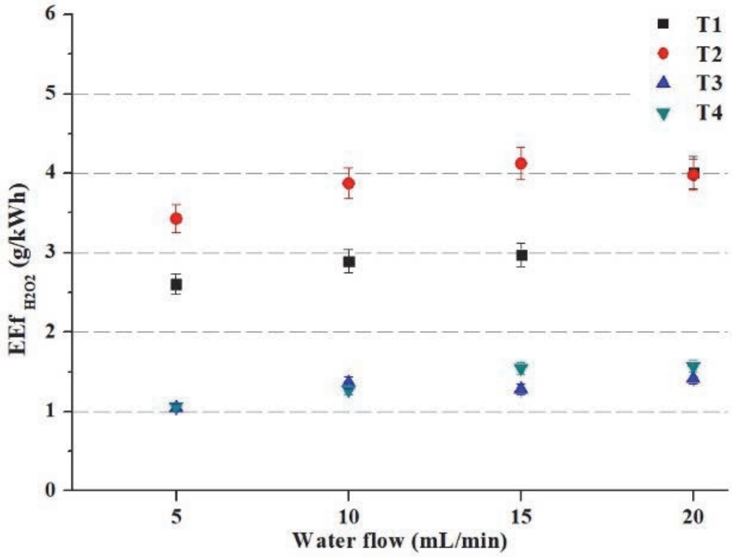

Fig. 8. Energy efficiency for H_2O_2 production for different T-NTP reactor configurations

Table 2. The energy efficiency of H_2O_2 production for T-NTP reactor configurations

Design	***H_2O [mL/min]***	***EEf $_{H2O2}$ [g/kWh]***					
		1 [L/min] Ar			***2 [L/min] Ar***		
		60	**150**	**250**	**60**	**150**	**250**
T1	5	3.2	1.7	1.5	3.5	3.9	2.6
	10	4.6	2.5	2.4	3.3	3.3	2.9
	15	6.9	2.3	2.7	3.6	3.5	3.0
	20	1.8	1.5	2.4	4.1	3.7	4.0
T2	5	3.9	2.9	3.1	3.8	2.4	3.4
	10	4.5	3.6	2.8	3.6	3.6	3.9
	15	6.2	5.2	3.9	3.6	3.8	4.1
	20	5.7	3.5	3.7	3.4	4.0	4.0
T3	5	3.2	2.4	0.8	1.0	1.1	1.0
	10	3.7	3.5	1.6	1.6	1.1	1.4
	15	3.1	4.0	1.3	2.0	1.4	1.3
	20	3.3	3.5	1.7	1.4	1.5	1.4
T4	5	0.9	0.7	0.7	1.0	0.6	1.1
	10	1.4	0.9	1.1	1.4	0.8	1.3
	15	1.3	0.8	1.0	1.6	0.8	1.5
	20	1.5	1.1	1.3	1.5	0.7	1.6

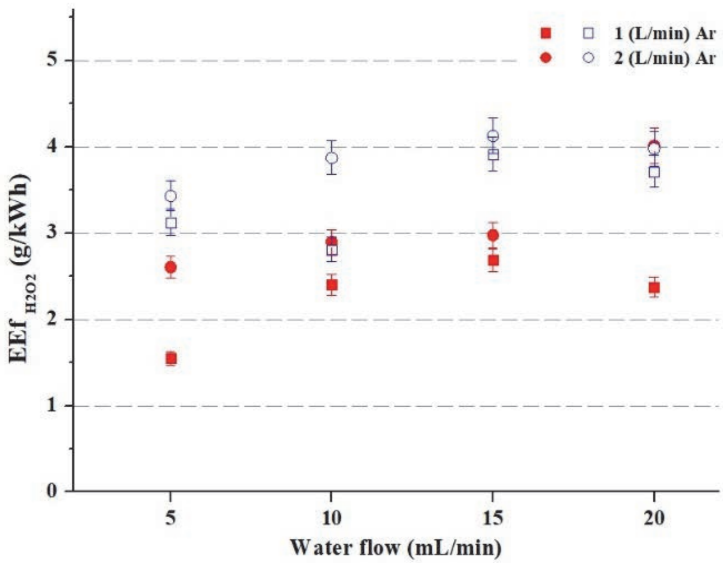

Fig. 9. Energy efficiency variation with water flow rate at 250 Hz T1 (■,●) and T2 (□,○)

The energy efficiency increases with the water flow rate, but not always the maximum value is reached at the highest water flow rate. This aspect is highlighted in Fig. 8 for the T2 configuration, where the maximum value of *EEf* is corresponding to a water flow rate of 15 mL/min. In Fig. 9, the influence of gas and water flow rates on energy efficiency, for T1 and T2, is emphasized.

The T2 configuration has the maximum values of *EEf* for the gas flow of 1 L/min, while the energy efficiency for the T1 configuration increases with the increase of the gas flow rate. As it can be noticed, the T2 configuration of the reactor ensures the highest values of energy efficiency.

4. Conclusions

This study presents the influence of the geometrical and electrical parameters of a NTP-T shaped reactor on hydrogen peroxide production. The evaluation was performed for different values of frequency (60, 150, and 250 Hz), water flow rates (5, 10, 15, and 20 mL/min) and gas flow rates (1 and 2 L/min Ar).

The reactive species generated in the T-NTP reactor depends on the geometry of the reactor but also on the electrical configuration of the electrodes. The highest values of H_2O_2 concentration and energy efficiency were obtained for the connections at which the discharge is generated between the water inlet electrode and the PAW outlet electrode (T1 and T2 design).

The H_2O_2 concentration decrease with the water flow rate and increases with the frequency. T2 reactor design ensures the highest values for energy efficiency of the considered T-NTP reactor designs for 1 L/min Ar. Instead, the T1 design, records the highest values for energy efficiency, at a gas flow rate of 2 L/min. T3 and T4 configurations have the lowest energy efficiency for hydrogen peroxide generation.

The reactor configuration and electrical parameters can be chosen accordingly to the requirements for PAW used in agriculture (greenhouses irrigation).

Acknowledgements

This paper was supported by the projects PN-III-P3-3.1-PM-RO-FR-2019-0213 (no. 19BM/2019), ERANET-MANUNET-III-Treatoflex (no. 146/2020) and PN-III-P2-2.1-PED-2019-0556 (no. 361PED/2020) within PNCDI III, financed by UEFISCDI.

References

Astanei D., Ursache M., Hnatiuc E., Stoica I., Hnatiuc B., Felea C., (2016), *Effects of GlidArc Plasma Treatment on Metallic Surface*, Proc. SPIE 10010, Advanced Topics in Optoelectronics, Microelectronics, and Nanotechnologies VIII, http://doi.org/10.1117/12.2243334.

Bafoil M., Jemmat A., Martinez Y., Merbahi N., Eichwald O., Dunand C., Yousfi M., (2018), Effects of low temperature plasmas and plasma activated waters on *Arabidopsis thaliana* germination and growth, *PloS one*, **13**, 0195512, doi:10.1371/journal.pone.0195512.

Bian W., Zhou M., Lei L., (2007), Formations of active species and by-products in water by pulsed high-voltage discharge, *Plasma Chemistry and Plasma Processing*, **27**, 337-348.

Brisset J.L., Fanmoe J., Hnatiuc E., (2016), Degradation of surfactant by cold plasma treatment, *Journal of Environmental Chemical Engineering*, **4**, 385-387.

Brisset, J. L., Moussa, D., Doubla, A., Hnatiuc, E., Hnatiuc, B., Youbi, K.G., Herry, J.-M., Naitali M., Bellon-Fontaine, N., (2008), Chemical reactivity of discharges and temporal post-discharges in plasma treatment of aqueous media: examples of gliding discharge treated solutions, *Industrial and Engineering Chemistry Research*, **47**, 5761-5781.

Burlica R., Dirlau I.D., Astanei D., (2019), Non-thermal mini-reactors for water treatment, *Environmental Engineering and Management Journal*, **18**, 1799-1807.

Burlica R., Grim R.G., Shih K.-Y., Balkwill D., Locke B.R., (2010), Bacteria inactivation using low power pulsed gliding arc discharges with water spray, *Plasma Processes and Polymers*, **7**, 640-649.

Burlica R., Hnatiuc B., Hnatiuc E., Ursache M., (2011), Effect of electrical current on H-2 / H_2O_2 generation in non-thermal plasma gliding arc reactors, *Environmental Engineering and Management Journal*, **10**, 579-583.

Clyne M., Coxon J., Setser D., Stedman D., (1969), Electronic excitation of OH and OD following collision of H_2, HCOOH and D_2O with metastable Ar (3P 2, 0) atoms, *Transactions of the Faraday Society*, **65**, 1177-1187.

Gomiero T., Paoletti M.G., Pimentel D., (2008), Energy and environmental issues in organic and conventional agriculture, *Critical Reviews in Plant Sciences*, **27**, 239-254.

Hnatiuc E., Astanei D., Ursache M., Hnatiuc B., Brisset J.L., (2012), *A review Over the Cold Plasma Reactors and their Applications*, Int. Conf. and Exposition on Electrical and Power Engineering, Iași, October 25-27, 497-502, http://doi.org/10.1109/icepe.2012.6463884.

Kramer A., Conway B.R., Meissner K., Scholz F., Rauch B.H., Moroder A., Ehlers A., Meixner A.J., Heidecke C.D., Partecke L.I., Kietzmann M., Assadian O., (2017), Cold atmospheric pressure plasma for treatment of chronic wounds: drug or medical device? *Journal of Wound Care*, **26**, 470-475.

Kriz P., Bartos P. et.al., (2016) Influence of plasma treatment in open air on mycotoxin content and grain nutriments, *Plasma Medicine*, **5**, 145-158.

Locke, B.R., Shih K.Y., (2011), Review of the methods to form hydrogen peroxide in electrical discharge plasma with liquid water, *Plasma Sources Science and Technology*, **20**, http://doi.org/10.1088/0963-0252/20/3/034006.

Moussa D., Brisset J.L., (2003), Disposal of spent tributylphosphate by gliding arc plasma, *Journal of Hazardous Materials*, **102**, 189-200.

Moussa D., Doubla A., Kamgang-Youbi G., Brisset J.L., (2007), Postdischarge long life reactive intermediates involved in the plasma chemical degradation of an azoic dye, *IEEE Transactions on Plasma Science*, **35**, 444-453.

Padureanu S., Stoleru V., Patras A., Burlica R., Dirlau D., Astanei D., Beniuga O., (2018), *Effect of Non-Thermal Activated Water on Lactuca Sativa L. Germination*

Dynamic, Int. Conf. and Exposition on Electrical and Power Engineering, 889-892.
Sera B., Gajdova I., Sery M., Spatenka P., (2013), New physicochemical treatment method of poppy seeds for agriculture and food industries, *Plasma Science and Technology*, **15**, 935-938.
Siddique M., Farooq R., Shaeen A., (2011), Removal of Reactive Blue 19 from wastewaters by physicochemical and biological processes – a review, *Journal of the Chemical Society of Pakistan*, **33**, 284 – 293.
Sivachandiran L., Khacef A., (2017), Enhanced seed germination and plant growth by atmospheric pressure cold air plasma: combined effect of seed and water treatment, *RSC Advances*, **7**, 1822-1832.
Stoleru V., Stratulat C., Teliban G., Padureanu S., Patras A., Burlica R., Dirlau D., Astanei D., Beniuga O., (2018), *Morphological, Physiological and Productive Indicators of Lettuce under Non-thermal Plasma*, Int. Conf. and Exposition on Electrical and Power Engineering, 937 - 942, http://doi.org/10.1109/ICEPE.2018.8559894.
Ursache M., Hnatiuc B., Hnatiuc E., Astanei D., Brisset J.L., Burlica R., (2015), Direct and delayed degradation of Azorubin (E122) by gliding arc discharges, *Environmental Engineering and Management Journal*, **14**, 2737-2746.
Vitousek P.M., Aber J.D., Howarth R.W., Likens G.E., Matson P.A., Schindler D.W., Schlesinger W.H., Tilman D., (1997), Human alteration of the global nitrogen cycle: Sources and consequences, *Ecological Applications*, **7**, 737-750.
Zadi T., Assadi A.A., Nasrallah N., Bouallouche R., Tri P.N., Bouzaza A., Azizi M.M., Maachi R., Wolbert D., (2018), Treatment of hospital indoor air by a hybrid system of combined plasma with photocatalysis: Case of trichloromethane, *Chemical Engineering Journal*, **349**, 276-286.